J Physiol Biochem (2015) 71:601–610
DOI 10.1007/s13105-015-0422-z

ORIGINAL PAPER

The isoforms generated by alternative translation initiation adopt similar conformation in the selectivity filter in TREK-2

Ren-Gong Zhuo · Peng Peng · Xiao-Yan Liu · Shu-Zhuo Zhang · Jiang-Ping Xu · Jian-Quan Zheng · Xiao-Li Wei · Xiao-Yun Ma

Received: 16 January 2015 / Accepted: 3 July 2015 / Published online: 14 August 2015

Abstract TREK-2 (TWIK-related K^+ channel-2), a member of two-pore domain potassium (K2P) channel family, tunes cellular excitability via conducting leak or background currents. In TREK-2, the isoforms generated by alternative translation initiation (ATI) mechanism exhibit large divergence in unitary conductance, but similar in selectivity to K^+. Up to now, the structural basis for this similarity in ion selectivity is unknown. Here, we report that externally applied Ba^{2+} inhibits the currents of TREK-2 in a concentration- and time-dependent manner. The blocking effect is blunted by elevated extracellular K^+ or mutation of S4 K^+ binding site, which suggests that the inhibitory mechanism of Ba^{2+} is due to its competitive docking properties within the selectivity filter (SF). Next, we demonstrate that all the ATI isoforms exhibit analogous behaviors upon the application of Ba^{2+} and alteration of extracellular pH (pH_o), which acts on the outer position of the SF. These results strongly support the notion that all the ATI isoforms of TREK-2 possess resembled SF conformation in S4 site and the position defined by pH_o, which implicates that neither the role of N-terminus (Nt) nor the unitary conductance is associated with SF conformation. Our findings might help to understand the detail gating mechanism of TREK-2 and K2P channels.

Keywords TREK-2 · Ba^{2+} · Selectivity filter · Alternative translation initiation · S4 K^+ binding site

Abbreviations

TREK	TWIK-related K^+ channel
K2P	Two-pore domain potassium channel
SF	Selectivity filter
ATI	Alternative translation initiation
Nt	N-terminus
pH_o	Extracellular pH
KcsA	Potassium channels from *S. lividans*
Kv channel	Voltage-gated K^+ channel
WT	Wild type

Introduction

TREK-2 (TWIK-related K^+ channel-2, K2P10.1) belongs to the two-pore domain potassium (K2P) channel family, which conducts leak or background currents that are essential to diverse cellular functions, including

R.-G. Zhuo · P. Peng · X.-Y. Liu · S.-Z. Zhang · J.-Q. Zheng · X.-L. Wei (✉) · X.-Y. Ma (✉)
State Key Laboratory of Toxicology and Medical Countermeasures, Department of Biochemical Pharmacology, Beijing Institute of Pharmacology and Toxicology, 27 Taiping Road, Beijing 100850, China
e-mail: weixl@bmi.ac.cn
e-mail: maxyer22@yahoo.com

P. Peng
Chinese PLA General Hospital, 28 Fuxing Street, Beijing 100853, China

J.-P. Xu
Department of Neuropharmacology, School of Pharmaceutical Sciences, Southern Medical University, No.1838, North Guangzhou Avenue, Guangzhou 510515, China

maintenance of the resting potential and regulation of excitability, sensory transduction, ion transport, cell volume metabolism, and apoptosis [13, 20]. The activity of the channel is sensitive to various physiological and pathological factors, such as neurotransmitters, hormones, temperature, unsaturated free fatty acids, mechanical stretch, intra- or extracellular pH, and protein kinases [1, 13, 20]. In addition, TREK-2 is also regulated by volatile general anesthetics, such as diltiazem and mibefradil [20, 24]. Accordingly, by tuning cellular excitability, the function of the channel is associated with diverse physiological, pathological, or pharmacological processes. For example, recent studies implicate that TREK-2 in dorsal root ganglion neurons hyperpolarizes C-nociceptors and limits pathological spontaneous pain [1].

Structurally, K2P channels are unique in that each subunit possesses four transmembrane segments and two pore-forming domains. As a result, mature K2P channels tend to form dimers to constitute the fourfold pore apparatus. Recent characterization of the crystal structures of two members of K2P channels reveals that the elements of pore structure are akin to other types of potassium channels. Along the ion conduction pathway in K2P channels, there also arranges the inner gate (activation gate) and selectivity filter (SF) gate (also called C-type gate, outer gate or inactivation gate) from intracellular side to extracellular side. Importantly, the structure of SF, which is formed by signature sequence TV(I)GY(F)G, is absolutely conserved among all K^+ channels [3, 23]. From extracellular side to intracellular side, the key carbonyl oxygens together with the side-chain hydroxyl oxygen of the threonines define four equally spaced K^+ binding sites, which are commonly termed as S1~S4 [2]. In the process of K^+ efflux, the SF experiences reversely conformational transition to produce conductive and non-conductive status alternately and highly discriminates K^+ over Na^+ eventually. Obviously, the SF plays a key role in gating the pore of K^+ channels, and thus, it is also referred as the SF gate [9, 10, 12, 13, 34, 35].

Alternative translation initiation (ATI) is an important cellular mechanism contributing to the diversity of protein functions. Accumulating evidence shows that the isoforms generated from ATI mechanism (ATI isoform) exhibits various functional properties [4, 21, 28, 30, 33]. TREK-1 is another member of TREK subclass, the nearest relative of TREK-2. It has been found that the TREK-1 ATI isoforms, which are different in the length of N-terminus (Nt), display a big diversity in both unitary conductance and K^+ selectivity [33]. By contrast, such ATI isoforms of TREK-2 only exhibit different conductance, whereas similar selectivity to K^+ [30]. According to previous study, the alteration of ion selectivity is associated with the SF conformational transition in TREK-1 [22], but whether such correlation also exists in TREK-2 is still unknown. Detailed sequence mapping shows that the intracellular Nt is involved in the regulation of unitary conductance level of TREK-2 channel [30]. However, whether the Nt affects the SF status of TREK-2 and the possible relationship between unitary conductance and SF conformation still remain to be explored. In this study, we report that Ba^{2+} inhibits TREK-2 currents by binding to the assumed K^+ binding site 4 (S4). Then, using Ba^{2+} and extracellular pH (pH_o) as SF gate probing tools, we reveal that all the ATI isoforms and wild-type (WT) TREK-2 display similar responses to the alterations of extracellular Ba^{2+} and pH_o, suggesting that they adopt roughly similar SF conformation in S4 site and the position affected by pH_o response. Accordingly, the resembled ion selectivity in ATI isoforms seems originated from their similar SF configuration, which seems support the idea that neither the SF conformation nor the role of Nt is involved in the regulation of the unitary conductance in TREK-2.

Materials and methods

Molecular biology

The cDNA encoding human TREK-2 (*NM*_138318.1) for this work was amplified from a TREK-2 plasmid (OriGene) by using PCR, and was cloned into pGH19 vector (a high-expression level vector in *Xenopus laevis* oocyte) using *Bgl*II(TaKaRa) and *Xba* I (TaKaRa), as described previously [22]. Mutants were produced using the MutanBEST kit (TaKaRa) according to the manufacturer's manual. All mutations were confirmed by DNA sequencing. cRNA was transcribed in vitro using the RiboMAX™ large-scale RNA production systems kit (Promega).

Electrophysiology

X. laevis were purchased from Nasco (USA). Oocytes were surgically removed from adult females and treated

with 0.5 mg/ml collagenase type II (Gibco, USA), defolliculated and incubated at 19 °C for 1~3 days before use. The oocytes were injected with ~5 ng cRNA (46 nl in volume) per cell. Whole-cell currents were measured 1~3 days after injection by the two-electrode voltage clamp technique, using an Axoclamp2B amplifier (Axon Instruments, Union City, CA). For two-electrode voltage clamp experiments, single oocyte was placed in a 0.3-ml perfusion chamber and impaled with two standard microelectrodes (1–2.5 MΩ resistance), which were filled with 3 M KCl. Recordings were performed in standard physiological extracellular solution, which contained (in mM): KCl, 5; NaCl, 93; $MgCl_2$, 1; $CaCl_2$,1.8; HEPES, 5; and adjusted to pH 7.4, with NaOH. HEPES buffer was replaced by Tris in pH 8.5–9.3 solutions and MES in pH 6.5 solutions. When required, potassium ions in bath solutions were isotonically replaced by sodium ions. $BaCl_2$ was diluted from 1 M stock and added to the various solutions as indicated. Recordings were performed under constant perfusion at room temperature. Oocyte membrane potential was held at −80 mV and currents were elicited by a ramp from −120 to +60 mV for 150 ms with a 2-s interpulse interval. Data were sampled at 2 kHz and filtered at 0.5 kHz with Clampex 10.2 software (Axon Instruments). The experiments were approved by the Animal Care and Ethics Committee of Southern Medical University and Beijing Institute of Pharmacology and Toxicology.

Data analysis

Concentration-response curves were fitted to the Hill equation according to the following parameters: $I=1/(1+([X]_o/IC_{50})^h)$, where I represents the recorded current, IC_{50} is the concentration of X (represents Ba^{2+} or H^+ in this research) required for achieving half-maximal effects, and h is the Hill coefficient. Time constants were calculated by fitting the data to the following equation: $I=I_o+A\times e-T/\tau$, where I is the current value, I_o is the inhibited current at equilibrium, T is the elapsed time after Ba^{2+} application, A is a constant and τ is the apparent forward time constant in seconds. The fitting was separately performed for each experiment using Origin 8.0 software (OriginLab).

Statistical significance was assessed with Student's t test using GraphPad Prism 5.0 (GraphPad Software, Inc.) software. A significant difference was considered when $p<0.05$.

Results

Ba^{2+} inhibits TREK-2 currents in a concentration- and time-dependent manner

Our previous studies indicate that Ba^{2+} inhibits the activity of TREK-1 channels [22]. TREK-1 and TREK-2 belong to the same subclass of K2P family and share 78 % homology at protein level [18]. We thus suspect that TREK-2 channels might display a similar response with TREK-1 upon the application of Ba^{2+}. To verify the hypothesis, we expressed TREK-2 channels in *X. laevis* oocytes, and the currents were elicited by voltage ramps from −120 to 60 mV. Indeed, as shown in Fig. 1a, on the application of increasing concentration of external Ba^{2+} ($[Ba^{2+}]_o$), the currents through TREK-2 channels were dramatically inhibited. At a test potential of 0 mV, the inhibition by the application of varied $[Ba^{2+}]_o$ was fitted by Hill equation. The half-maximal inhibitory concentration (IC_{50}) and Hill coefficient were estimated to be 0.84±0.06 mM and 1.61±0.12, respectively (Fig. 1b). The Hill coefficient was bigger than 1, implicating that the interaction between TREK-2 and Ba^{2+} is positively cooperative.

Moreover, Ba^{2+} blockade on TREK-2 was time dependent. At the presence of 1 mM Ba^{2+}, the currents were decreased gradually as the time elapsed until the steady-state blockade was achieved. When washout was performed, the activity of TREK-2 was also gradually recovered (Fig. 1c). As $[Ba^{2+}]_o$ was enhanced to 2 and 4 mM, the binding rate of the ions was accelerated (Fig. 1d). The time course of blocking was fitted with a mono exponential function, and the apparent forward time constant for Ba^{2+} inhibition (τ_{block}) was estimated. When the $[Ba^{2+}]_o$ was increased from 0.5 to 6 mM, the τ_{block} decreased from 40.86±3.82 to 13.77±0.75 s (Fig. 1E, $p<0.01$). However, we did not observe the correlation between exit rate of Ba^{2+} and its concentration (data not shown). Taken together, above data clearly demonstrate that Ba^{2+} inhibits the currents of TREK-2 channels in a concentration- and time-dependent manner.

External K^+ blunts the blocking effect of Ba^{2+} on TREK-2

It has been established that Ba^{2+} has a similar radius as K^+ and is able to block the activity of several types of potassium channels through fitting into the selectivity

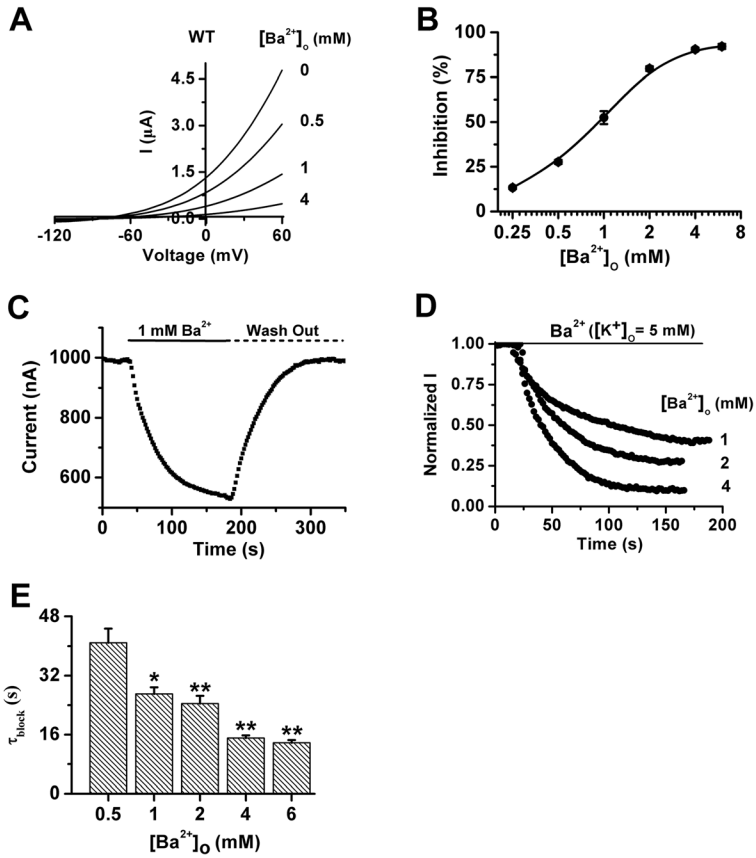

Fig. 1 TREK-2 currents are inhibited by externally applied Ba^{2+} in a concentration- and time-dependent manner. **a** Representative current–voltage relationship for TREK-2 expressed in *Xenopus* oocytes in the absence and presence of different $[Ba^{2+}]_o$. The concentration of extracellular K^+ was 5 mM. Currents were elicited by a voltage ramp from −120 to 60 mV, from a holding potential of −80 mV. **b** Dose response for inhibition of wild-type TREK-2 (WT) channels at 0 mV with the protocol in A. Data points were mean±SE ($n \geq 6$). The *solid line* represents the best fit of the data to the Hill equation. **c** The time course of binding and unbinding of 1 mM Ba^{2+} to TREK-2 channel from a representative TREK-2-expressing oocyte. **d** The time course of inhibition to TREK-2 channel by different $[Ba^{2+}]_o$ from a representative TREK-2-expressing oocyte. **e** The time constant (τ_{block}, s) of inhibition to TREK-2 current by different $[Ba^{2+}]_o$ (mean±SE, n≥6). *p<0.05 or **p<0.01 versus 0.5 mM $[Ba^{2+}]_o$

filter (SF) [7, 14, 25]. If that is also the case in TREK-2, the effects of Ba^{2+} could be blunted by elevated concentration of extracellular K^+ ($[K^+]_o$) [8, 22, 26, 27]. To address this hypothesis, the access degree of Ba^{2+} to the channel in different $[K^+]_o$ was assessed. As the time-dependent curves illustrated in Fig. 2a, enhancement of $[K^+]_o$ from 0 to 40 mM dramatically interfered Ba^{2+} binding to TREK-2. As a result, the ability of 1 mM $[Ba^{2+}]_o$ to block TREK-2 was blunted from 96.26± 0.27 % at K^+-free condition to 52.48±3.61, 21.57± 1.99, and 10.66±1.69 % at 5, 20, and 40 mM $[K^+]_o$, respectively. These results reveal that the binding of Ba^{2+} to TREK-2 channels is strongly affected by $[K^+]_o$, which implicates that the binding site of Ba^{2+} may reside within the SF of TREK-2.

Ba^{2+} blocks TREK-2 by binding at the S4 site within the selectivity filter

Variation of $[K^+]_o$ is tightly coupled to conformational change at SF, i.e., K^+-free extracellular solution evokes a non-conductive state of SF [35]. Since Ba^{2+} binding to TREK-2 is associated with such K^+-dependent SF conformational transition and, especially, Ba^{2+} blocks TREK-1 by overlapped binding at the S4 site within SF [22], we next investigated whether the ions bind to the S4 site of TREK-2. The putative threonines (positions 172 and 281) comprising the S4 site of TREK-2 are strictly conserved compared with several types of K^+ channels (Fig. 3a). To test our hypothesis, mutants containing the threonine-to-serine

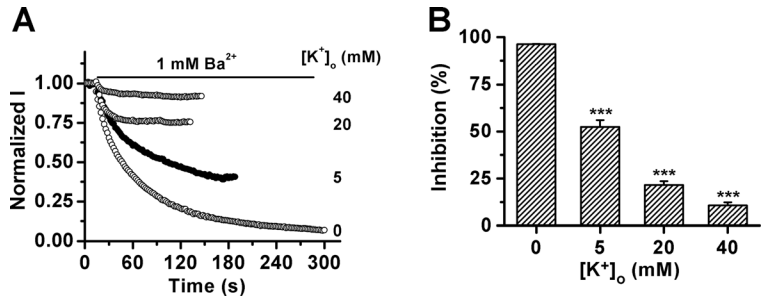

Fig. 2 Effects of different $[K^+]_o$ on Ba^{2+} inhibition of TREK-2 currents. **a** Effects of different $[K^+]_o$ on the time course of blockade by 1 mM Ba^{2+} in a representative oocyte expressing TREK-2 channels. **b** Average TREK-2 current decreased by Ba^{2+} (in %) in different $[K^+]_o$. Data represent mean±SE ($n \geq 6$). ***$p<0.01$ versus 0 mM $[K^+]_o$

transition at positions 172 (T172S) and 281 (T281S) were constructed. As the time-dependent curves shown in Fig. 3b, the response of the mutants to 2 mM $[Ba^{2+}]_o$ were drastically blunted. Accordingly, the IC_{50} for Ba^{2+} block to T172S and T281S was 5.32±1.27 and 4.9±0.65 mM, respectively (Fig. 3c). Obviously, the threonine mutations increased the IC_{50} for Ba^{2+} by approximately sixfolds, suggesting that Ba^{2+} blocks TREK-2 currents by occupying theS4 site within SF.

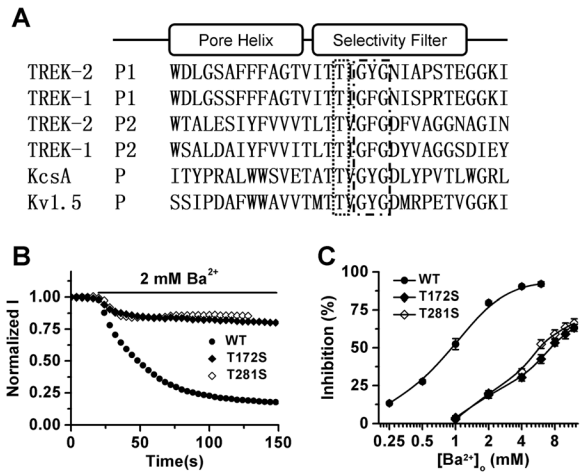

Fig. 3 Ba^{2+} inhibits TREK-2 current through binding at S4 site of the selectivity filter. **a** Multiple sequences alignment of the SF regions of TREK-2 (P1 and P2), TREK-1(P1 and P2), KcsA, and Kv1.5. The positions of the conserved threonine residues among them and the SF GY/FG signature sequences were boxed. **b** Comparison of the relative 2 mM Ba^{2+} inhibitory effects on WT, the T172S mutant, and the T281S mutant. The currents recorded from representative oocytes expressing the indicated channels. **c** Dose–response curves of the WT, T172S, and T281S mutants. Data points were mean±SE ($n \geq 6$). The data were fitted with Hill equation

The isoforms generated by alternative translation initiation (ATI isoform) mechanism adopts similar conformation in S4 site

Because of "leaky scanning" of ribosomes to initiation site [16], mRNA of TREK-2 channels generates three isoforms (Fig. 4a). These isoforms display largely divergent conductance, but exhibit similar selectivity for K^+ [30]. Given that the SF configuration of K^+ channels is directly associated with ion selectivity, we thus suspect that the ATI isoforms might have similar conformation in SF. As established above, Ba^{2+} inhibits TREK-2 activity through docking at S4 site, and thus, these alkaline metal ions could be used as specific tools to define the conformational alteration in S4 site. We then measured the Ba^{2+} response of ATI isoforms.

Mutants were constructed such that only one specific initiation site could be used, as described previously [30]. The wild-type human TREK-2 was referred as WT (also termed as $M_1M_2M_3$). The M_2L_3 were constructed by deleting the segment before the second initiation site and mutating the third initiation site to leucine simultaneously. The Nt up to the third initiation site was deleted to produce M_3. Both of the second and third methionines (M_2 and M_3) were mutated to leucines simultaneously to generate $M_1L_2L_3$ (Fig. 4a). As shown in Fig. 4b, the concentration response curves for all the mutants displayed similar Ba^{2+} blocking profile with those of WT channels. Accordingly, their IC_{50}s did not show significant change compared with WT channels, with a value of 0.95±0.11, 0.91±0.02, and 0.96±0.05 mM for M_2L_3,M_3 and $M_1L_2L_3$, respectively (Fig. 4c, $p>0.05$). Moreover, in the presence of different $[Ba^{2+}]_o$, no significant difference was found in the access and exit rate of Ba^{2+} ($\tau_{unblock}$, calculated by

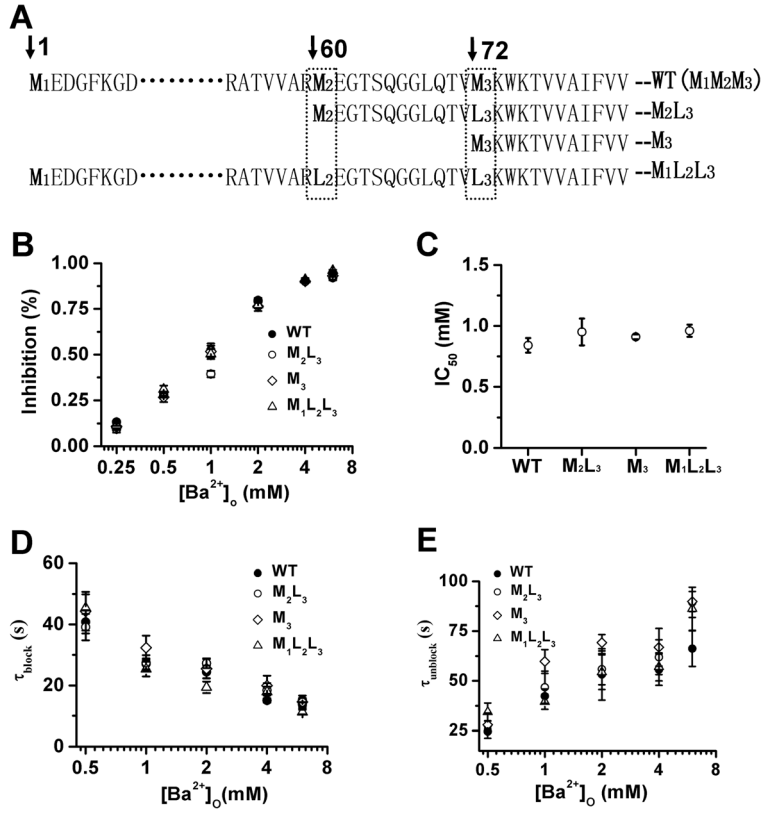

Fig. 4 Response of TREK-2 isoforms generated by ATI mechanism to externally applied Ba^{2+}. **a** The Nt sequence of the ATI isoforms (WT and M_3) and the mutants that harboring the M-to-L transition of the second and/or third initiation sites (M_2L_3 and $M_1L_2L_3$). The potential initiation sites located at positions 1, 60, and 72 were boxed. **b** Comparison of the inhibition percentage for the indicated channels in the presence of varying $[Ba^{2+}]_o$. Data points were mean±S.E ($n \geq 6$). **c** IC_{50} values of $[Ba^{2+}]_o$ inhibition for TREK-2 isoforms and mutated channels. **d** The access rate (τ_{block}, s) of Ba^{2+} to TREK-2 isoforms and mutants at different $[Ba^{2+}]_o$ (mean±SE, $n \geq 5$). **e** The exit rate ($\tau_{unblock}$, s) of Ba^{2+} to TREK-2 isoforms and mutants at different $[Ba^{2+}]_o$ (mean±SE, $n \geq 5$)

fitting the data to mono exponential equation) between WT channels and ATI isoforms (Fig. 4d, e, $p > 0.05$). These resembled behaviors of ATI isoforms upon the application of Ba^{2+} demonstrate that they roughly adopt similar conformation in the S4 site. In addition, these results suggest that the Nt domain is not involved in the regulation of the conformational transition in S4 site.

The ATI isoforms experience similar conformational transitions induced by extracellular H^+ within SF

TREK-1, the nearest relative of TREK-2 in K2P family, is inhibited by extracellular acidification via a mechanism resembling C-type inactivation [8]. Both crystal structural analysis of KcsA (potassium channels from *S. lividans*) [11] and functional characterization of other K^+ channels [12, 22, 31, 37, 38] indicate that structural collapse (or barrier formation) occurs at the outer of SF during C-type inactivation. TREK-2 is also inhibited by alkaline pH_o, and these effects are blunted by high $[K^+]_o$ [29], which implicates that pH_o modulates TREK-2 via manipulating SF. Despite that the His151 has been identified as a pH_o sensor [29], the relative location of SF involved in the regulation (pH_o position) is still unknown. Thus, to define the possible relationship between the relative position regulated by pH_o and S4 site, we further evaluated the response of S4 site mutants to alteration of pH_o. S4 is the innermost site of SF; hence, if pH_o acts on the S4 site or inner part of SF, the response of S4 mutants to pH_o will be altered. However, under physiological potassium concentration (5 mM), the degree of pH_o effects was resembled between S4 mutants and WT channels (Fig. 5a). The fitting to Hill equation revealed a half block (pH_{50}) of 7.67±0.35, 8.12±0.09, and 7.95±0.12 for WT, T172S, and T281S, respectively (Fig. 5b, $p > 0.05$). Since mutations of S4 site do not affect pH_o response of TREK-2 channels, the conformational transition evoked by pH_o fluctuation is other than the S4 site, that is, the outer position of SF.

Next, we investigated whether the ATI isoforms possess similar conformation in outer SF by examining the pH_o response of the Nt mutants. Firstly, the gradual current loss induced by pH_o elevation from 6.5 to 9.3 in the representative oocytes expressing WT channel and $M_1L_2L_3$, one of ATI isoform, was very similar

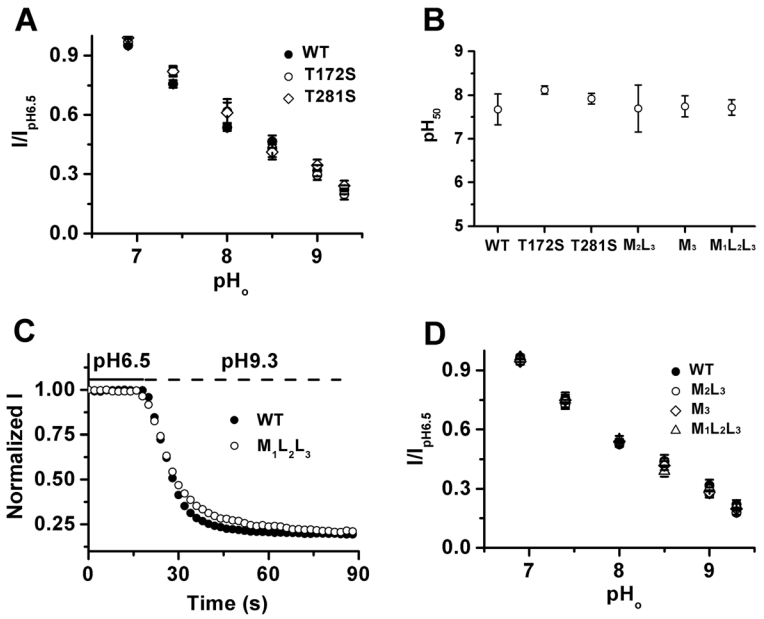

Fig. 5 Response of ATI isoforms and mutants to extracellular fluctuation of pH. **a** Normalized responses of the indicated WT and S4 site mutated channels to pH_o changes in 5 mM $[K^+]_o$ solution. Data (mean±SE, $n \geq 6$) was taken at 0 mV, normalized to activity at pH 6.5. **b** Summary of the pH_{50} values for pH inhibition of the indicated TREK-2 channels. Results were shown to as mean±SE ($n \geq 5$). **c** Exemplar recordings of the response of WT channels and $M_1L_2L_3$ mutant to the external pH_o changes from 6.5 to 9.3. The currents recorded in pH 9.3 were normalized by those recorded in pH 6.5. **d** Comparison of the pH_o response between ATI isoforms and related mutants. Data (mean±SE, $n \geq 6$) was taken at 0 mV, normalized to activity at pH 6.5

(Fig. 5c). Further measurement of the response all the Nt mutants to varied pH_o (Fig. 5d) revealed that the pH_{50} for M_2L_3, M_3, and $M_1L_2L_3$ was 7.70±0.54, 7.74±0.24, and 7.72±0.18, respectively, a similar range with WT channels (Fig. 5b, $p > 0.05$). The resembled pH_o response between WT channels and Nt mutants demonstrate that the outer SF conformation of ATI isoforms (the position was termed as pH_o position in this study) is similar with that of WT channels.

Taken together, our provided data indicate that the SF conformations of ATI isoforms and WT TREK-2 are similar in the S4 site and pH_o position, suggesting the role of Nt domain is not associated with the conformation of SF. Since the domain controls the single-channel conductance [30], it seems that the conformational alteration of SF does not contribute to unitary conductance of TREK-2.

Discussion

Ba^{2+} has been proven to be a valuable tool to learn about the SF configuration of K^+ channels, due to its ability to prevent the K^+ flux effectively in several types of K^+ channels through fitting into the SF [5, 6, 14, 22, 25]. Using Ba^{2+} as a probe, we have previously confirmed that extracellular K^+-free and acidification induce collapsed SF conformation in TREK-1 [22]. Here, by detail characterizing the interaction between Ba^{2+} and TREK-2 channels, we demonstrate that the ions are also capable of blocking TREK-2 expressed in *X. laevis* oocytes, in a concentration- and time-dependent manner (Fig. 1). The inhibition is blunted by elevated $[K^+]_o$, strongly suggesting that Ba^{2+} exerts its inhibitory function to TREK-2 via acting on the SF gate (Fig. 2). The decreased sensitivity of S4 site mutants (T172S and T281S) to the application of Ba^{2+} provides further evidence that the ion binds at S4 site of TREK-2 (Fig. 3). The regulation mode of Ba^{2+} to TREK-2 supports the notion that the SF is highly conserved between TREK-2 and other types of K^+ channels, as illustrated in the crystal structures of K2P channels [3, 23]. Moreover, Ba^{2+} is also a qualified tool to explore the properties of the SF in TREK-2 channels.

Except for Ba^{2+}, we also investigated the effects of pH_o, which is considered as another input modality that acts on the SF of TREK-2. TREK-1 is inhibited by acidic pH_o via a mechanism resembling C-type

inactivation, in which the structure of outer SF is collapsed [8, 22]. In contrast to the situation of TREK-1, the activity of TREK-2 is inhibited by alkaline pH_o [29]. Elevated $[K^+]_o$ impedes the inhibition [29, 36], which suggests that pH_o also acts on the SF of TREK-2 channels. We reveal that destruction of S4 site does not alter the sensitivity of TREK-2 to pH_o (Fig. 5a, b), which implicates that the conformational transition induced by pH_o occurs at the location (pH_o position) where is different from S4 site. As S4 is the innermost K^+ binding site, the pH_o position should be located at the outer SF, which is consistent with the concept that C-type inactivation involves a localized constriction in the outer vestibule of the selectivity filter. Structural analysis of KcsA reveals that S2 and S3 are lost in the SF configuration of C-type inactivation [11], whereas functional characterization of TASK2 (TWIK-related acid-sensitive potassium channel 2, another member of K2P family) indicates that the energetic barriers at S0/S1 account for channel blockade at acid pH_o [38]. The outer SF regulation properties enable pH_o to be another facile tool to explore the characteristics of other stimuli that act on the SF of TREK-2 channels.

Cloned rat and human TREK-2 expressed in mammalian cells and in *Xenopus* oocytes exhibits multiple unitary conductance levels that range from ~52 to ~220 pS [15, 30]. Nt participates in the regulation of conductance, as illustrated by the behavior of the three ATI isoforms. Full length isoform has small unitary conductance near 52 pS, while short isoforms translated from the second and third initiation sites have large conductance between 185 and 220 pS. Using extracellular Ba^{2+} and pH_o as tools, we investigated whether the Nt commands the conductance via controlling the SF conformation. In the presence of different $[Ba^{2+}]_o$, all the ATI isoforms exhibit similar response, including the access rate, exit rate, and inhibition ratio (Fig. 4). Obviously, the Nt does not affect Ba^{2+} binding to TREK-2, which suggests the all the ATI isoforms have similar S4 configuration, and the Nt does not influence the S4 conformation. Moreover, we also evaluated the response of all the ATI isoforms to varied pH_o. Very similar to the situation of Ba^{2+}, the isoforms also display analogous responses to pH_o (Fig. 5c, d). Since pH_o acts on the outer vestibule of the SF, we conclude that all the ATI isoforms possess similar outer SF conformation. Together, these data strongly implicate that all the ATI isoforms and WT channels show similar conformation in their SF region, and the Nt of TREK-2 channels is not associated with the SF conformation. We then speculate that in TREK-2 channels, the conformation of the SF has no impact on the single-channel conductance. This concept is in accordance with the phenomenon that all the ATI isoforms possess different conductance but exhibit similar selectivity to K^+ [30]. In voltage-gated K^+ (Kv) channels, residue substitutes in the vicinity of inner gate or replacement the inner helices (constitute the inner gate) affect the unitary conductance, whereas exchanging the SF between shaker and Kv3.1 does not influence the conductance [19, 32]. These results implicate that the unitary conductance is highly associated with the status of the inner gate [17]. Hence, the SF configuration is mainly conserved to control the selectivity to K^+ and to allow K^+ flow, rather than regulating the conductance. Our data regarding the function of SF on unitary conductance in TREK-2 channels appear resembled with those of Kv channels. However, this property is not necessarily identical among all the K^+ channels, even in the TREK subclass of K2P channels. For example, ATI isoforms of TREK-1 channels also show big divergence in unitary conductance, but the Nt deletant [33], one of the ATI isoforms, displays nonconductive SF conformation compared with its wild-type counterpart [22]. And accordingly, the selectivity for K^+ ions of the truncated channels is decreased [33].

In addition to identical selectivity to K^+ among TREK-2 isoforms, these isoforms also have similar sensitivity to activators and inhibitors such as arachidonic acid, membrane stretch, proton, and cAMP. It has been established in TREK-1 channels that the active sites of these stimuli is gathered within the proximal region of intracellular C-terminus [13, 20], a relatively highly conserved region between TREK-1 and TREK-2. Therefore, it is easy to understand that the active sites of these input modalities could also be located within the proximal side of the C-terminus. Consequently, all the ATI isoforms have completely identical C-terminus, which might lead to their similar response to above stimuli.

In summary, we found that externally, application of Ba^{2+} inhibits TREK-2 currents in a time- and concentration-dependent manner. The blocking effects are blunted by elevated $[K^+]_o$ and mutations of S4 site, suggesting the inhibitory mechanism of the ion is originated from its docking properties within the SF. Furthermore, we identified that pH_o acts on the position outer of S4 site. Then, using extracellular Ba^{2+} and pH_o as probing tools, we demonstrate that TREK-2 isoforms

generated by ATI mechanism adopts similar conformation in S4 site and the pH_o position, implicating that the Nt has a minor effect, if any, on regulating the SF conformation. We thus speculate the SF conformation plays a little role on the single-channel conductance in TREK-2 channels. Our findings characterize the relation between the Nt and the SF status, which may help to understand the detail gating mechanism of TREK-2 channels and K2P channels.

Acknowledgments We thank Professor Gail Robertson (University of Wisconsin-Madison Medical School, Madison, WI) for the pGH-19 plasmid.

Grants This work was supported by grants from National Major Scientific and Technological Special Project for "Significant New Drug Development" (2014ZX09507-003), National Integrated Drug Discovery Technology Platform Foundation of China (2012ZX09301003-001), and the National Science Foundation of China Grants (31200797).

References

1. Acosta C, Djouhri L, Watkins R, Berry C, Bromage K, Lawson SN (2014) TREK2 expressed selectively in IB4-binding C-fiber nociceptors hyperpolarizes their membrane potentials and limits spontaneous pain. J Neurosci 34:1494–1509
2. Berneche S, Roux B (2001) Energetics of ion conduction through the K+ channel. Nature 414:73–77
3. Brohawn SG, Del MJ, MacKinnon R (2012) Crystal structure of the human K2P TRAAK, a lipid- and mechano-sensitive K+ ion channel. Science 335:436–441
4. Cai J, Huang Y, Li F, Li Y (2006) Alteration of protein subcellular location and domain formation by alternative translational initiation. Proteins 62:793–799
5. Chang HK, Marton LJ, Liang KK, Shieh RC (2009) K+ binding in the G-loop and water cavity facilitates Ba2+ movement in the Kir2.1 channel. Biochimica et biophysica acta 1788:500–506
6. Chatelain FC, Alagem N, Xu Q, Pancaroglu R, Reuveny E, Minor DL Jr (2005) The pore helix dipole has a minor role in inward rectifier channel function. Neuron 47:833–843
7. Chatelain FC, Gazzarrini S, Fujiwara Y, Arrigoni C, Domigan C, Ferrara G, Pantoja C, Thiel G, Moroni A, Minor DL Jr (2009) Selection of inhibitor-resistant viral potassium channels identifies a selectivity filter site that affects barium and amantadine block. PLoS One 4, e7496
8. Cohen A, Ben-Abu Y, Hen S, Zilberberg N (2008) A novel mechanism for human K2P2.1 channel gating. Facilitation of C-type gating by protonation of extracellular histidine residues. J Biol Chem 283:19448–19455
9. Cordero-Morales JF, Cuello LG, Zhao Y, Jogini V, Cortes DM, Roux B, Perozo E (2006) Molecular determinants of gating at the potassium-channel selectivity filter. Nat Struct Mol Biol 13:311–318
10. Cordero-Morales JF, Jogini V, Lewis A, Vasquez V, Cortes DM, Roux B, Perozo E (2007) Molecular driving forces determining potassium channel slow inactivation. Nat Struct Mol Biol 14:1062–1069
11. Cuello LG, Jogini V, Cortes DM, Perozo E (2010) Structural mechanism of C-type inactivation in K(+) channels. Nature 466:203–208
12. Domene C, Klein ML, Branduardi D, Gervasio FL, Parrinello M (2008) Conformational changes and gating at the selectivity filter of potassium channels. J Am Chem Soc 130:9474–9480
13. Enyedi P, Czirjak G (2010) Molecular background of leak K+ currents: two-pore domain potassium channels. Physiol Rev 90:559–605
14. Jiang Y, MacKinnon R (2000) The barium site in a potassium channel by x-ray crystallography. J Gen Physiol 115:269–272
15. Kang D, Choe C, Cavanaugh E, Kim D (2007) Properties of single two-pore domain TREK-2 channels expressed in mammalian cells. J Physiol 583:57–69
16. Kozak M (2005) Regulation of translation via mRNA structure in prokaryotes and eukaryotes. Gene 361:13–37
17. Labro AJ, Snyders DJ (2012) Being flexible: the voltage-controllable activation gate of kv channels. Front Pharmacol 3:168
18. Lesage F, Terrenoire C, Romey G, Lazdunski M (2000) Human TREK2, a 2P domain mechano-sensitive K+ channel with multiple regulations by polyunsaturated fatty acids, lysophospholipids, and Gs, Gi, and Gq protein-coupled receptors. J Biol Chem 275:28398–28405
19. Lopez GA, Jan YN, Jan LY (1994) Evidence that the S6 segment of the Shaker voltage-gated K+ channel comprises part of the pore. Nature 367:179–182
20. Lotshaw DP (2007) Biophysical, pharmacological, and functional characteristics of cloned and native mammalian two-pore domain K+ channels. Cell Biochem Biophys 47:209–256
21. Lu NZ, Cidlowski JA (2005) Translational regulatory mechanisms generate N-terminal glucocorticoid receptor isoforms with unique transcriptional target genes. Molecular cell 18:331–342
22. Ma XY, Yu JM, Zhang SZ, Liu XY, Wu BH, Wei XL, Yan JQ, Sun HL, Yan HT, Zheng JQ (2011) External BA2+ block of two-pore-domain potassium channel trek-1 defines conformational transition in its selectivity filter. J Biol Chem.
23. Miller AN, Long SB (2012) Crystal structure of the human two-pore domain potassium channel K2P1. Science 335:432–436
24. Noel J, Sandoz G, Lesage F (2011) Molecular regulations governing TREK and TRAAK channel functions. Channels (Austin) 5
25. O'Connell AD, Morton MJ, Sivaprasadarao A, Hunter M (2005) Selectivity and interactions of Ba2+ and Cs+ with wild-type and mutant TASK1 K+ channels expressed in Xenopus oocytes. J Physiol 562:687–696
26. Ogielska EM, Aldrich RW (1999) Functional consequences of a decreased potassium affinity in a potassium channel pore. Ion interactions and C-type inactivation J Gen Physiol 113:347–358
27. Piechotta PL, Rapedius M, Stansfeld PJ, Bollepalli MK, Erhlich G, Andres-Enguix I, Fritzenschaft H, Decher N,

Sansom MS, Tucker SJ et al (2011) The pore structure and gating mechanism of K2P channels. EMBO J 30:3607–3619
28. Rhen T, Cidlowski JA (2005) Antiinflammatory action of glucocorticoids—new mechanisms for old drugs. The New England journal of medicine 353:1711–1723
29. Sandoz G, Douguet D, Chatelain F, Lazdunski M, Lesage F (2009) Extracellular acidification exerts opposite actions on TREK1 and TREK2 potassium channels via a single conserved histidine residue. Proc Natl Acad Sci U S A 106: 14628–14633
30. Simkin D, Cavanaugh EJ, Kim D (2008) Control of the single channel conductance of K2P10.1 (TREK-2) by the amino-terminus: role of alternative translation initiation. J Physiol 586:5651–5663
31. Stansfeld PJ, Grottesi A, Sands ZA, Sansom MS, Gedeck P, Gosling M, Cox B, Stanfield PR, Mitcheson JS, Sutcliffe MJ (2008) Insight into the mechanism of inactivation and pH sensitivity in potassium channels from molecular dynamics simulations. Biochemistry 47:7414–7422
32. Taglialatela M, Champagne MS, Drewe JA, Brown AM (1994) Comparison of H5, S6, and H5-S6 exchanges on pore properties of voltage-dependent K+ channels. J Biol Chem 269:13867–13873
33. Thomas D, Plant LD, Wilkens CM, McCrossan ZA, Goldstein SA (2008) Alternative translation initiation in rat brain yields K2P2.1 potassium channels permeable to sodium. Neuron 58: 859–870
34. Wang DT, Hill AP, Mann SA, Tan PS, Vandenberg JI (2011) Mapping the sequence of conformational changes underlying selectivity filter gating in the K(v)11.1 potassium channel. Nat Struct Mol Biol 18:35–41
35. Zhou Y, Morais-Cabral JH, Kaufman A, MacKinnon R (2001) Chemistry of ion coordination and hydration revealed by a K+ channel-Fab complex at 2.0 A resolution. Nature 414:43–48
36. Zhuo RG, Liu XY, Zhang SZ, Wei XL, Zheng JQ, Xu JP, Ma XY (2015) Insights into the stimulatory mechanism of 2-aminoethoxydiphenyl borate on TREK-2 potassium channel. Neuroscience 300:85–93
37. Zilberberg N, Ilan N, Goldstein SA (2001) KCNKO: opening and closing the 2-P-domain potassium leak channel entails "C-type" gating of the outer pore. Neuron 32:635–648
38. Zuniga L, Marquez V, Gonzalez-Nilo FD, Chipot C, Cid LP, Sepulveda FV, Niemeyer MI (2011) Gating of a pH-sensitive K(2P) potassium channel by an electrostatic effect of basic sensor residues on the selectivity filter. PLoS One 6:e16141